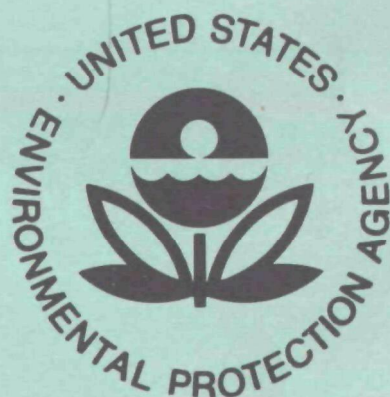


**EPA-600/3-77-028**

**March 1977**

**Ecological Research Series**

# **HETEROGENEOUS REACTIONS OF NITROGEN OXIDES IN SIMULATED ATMOSPHERES**



**Environmental Sciences Research Laboratory  
Office of Research and Development  
U.S. Environmental Protection Agency  
Research Triangle Park, North Carolina 27711**

EPA-600/3-77-028  
March 1977

HETEROGENEOUS REACTIONS OF NITROGEN OXIDES  
IN SIMULATED ATMOSPHERES

by

H.S. Judeikis, S. Siegel, T.B. Stewart and H.R. Hedgpeth  
The Aerospace Corporation  
El Segundo, California 90245

R802687-01

Project Officer

Jack L. Durham  
Atmospheric Chemistry and Physics Division  
Environmental Sciences Research Laboratory  
Research Triangle Park, North Carolina 27711

ENVIRONMENTAL SCIENCES RESEARCH LABORATORY  
OFFICE OF RESEARCH AND DEVELOPMENT  
U.S. ENVIRONMENTAL PROTECTION AGENCY  
RESEARCH TRIANGLE PARK, NORTH CAROLINA 27711

## DISCLAIMER

This report has been reviewed by the Environmental Sciences Research Laboratory, U.S. Environmental Protection Agency, and approved for publication. Approval does not signify that the contents necessarily reflect the views and policies of the U.S. Environmental Protection Agency, nor does mention of trade names of commercial products constitute endorsement or recommendation for use.

## ABSTRACT

A laboratory study has been conducted on heterogeneous reactions of nitrogen dioxide and nitric oxide to evaluate their potential role in reactions in polluted urban atmospheres. The results of this study suggest that nitrogen dioxide decomposes on a wide variety of solids likely to be found in urban environments. Measured reaction rates indicate these processes can be important in the atmosphere. Humidification of reaction mixtures leads to increased reactivities. It is concluded that heterogeneous reactions in the atmosphere are unimportant for the oxidation of nitric oxide.

This report was submitted in fulfillment of Grant No. R-802687-01 by the Aerospace Corporation under the partial sponsorship of the U.S. Environmental Protection Agency. This report covers a period from November 1973 to November 1976, and work was completed as of November 1976.

## CONTENTS

Abstract . . . . .	iii
Figures and Tables . . . . .	vi
1. Introduction . . . . .	1
2. Experimental . . . . .	3
Materials . . . . .	3
Reactors . . . . .	3
Analysis of surface nitrogen compounds . . . . .	6
3. Results . . . . .	7
Decomposition of $\text{NO}_2$ in dry reaction mixtures . . . . .	7
Decomposition of $\text{NO}_2$ in moist reaction mixtures . . . . .	16
Reactivity of NO . . . . .	21
4. Discussion and Conclusions . . . . .	22
References . . . . .	24

## FIGURES

<u>Number</u>		<u>Page</u>
1	Decomposition of $\text{NO}_2$ over charcoal . . . . .	8
2	Decomposition of $\text{NO}_2$ over $\text{MnO}_2$ . . . . .	10
3	Decomposition of $\text{NO}_2$ over $\text{PbO}$ and cement . . . . .	12
4	Surface nitrogen compounds measured after $\text{NO}_2$ decomposition over $\text{Al}_2\text{O}_3$ . . . . .	17
5	Decomposition of $\text{NO}_2$ over $\text{Al}_2\text{O}_3$ . . . . .	18
6	Decomposition of $\text{NO}_2$ over selected solids . . . . .	19

## TABLES

1	Solids studied and physical adsorption surface areas . . . . .	4
2	Decomposition of $\text{NO}_2$ over charcoal . . . . .	9
3	Decomposition of $\text{NO}_2$ over various solids . . . . .	14
4	Analysis of surface nitrogen compounds . . . . .	15

## SECTION 1

### INTRODUCTION

In recent years, considerable attention has been given to the study of aerosols in polluted urban atmospheres. This interest has arisen because of potential health effects, as well as the possibility that aerosols may play an active role in the physical and chemical processes taking place in the atmosphere. A well-known example of the latter phenomena is the oxidation of sulfur dioxide in water droplets (1-4).

Previously, through the use of a simple model and data from the catalyst literature, the conditions were outlined under which selected heterogeneous reactions involving urban aerosols could compete with gas phase reactions that are known or are postulated to occur (5). Although the model calculations suggested heterogeneous reactions could compete with homogeneous gas phase reactions, the major limitation to these conclusions lay in the fact that the literature data used were generally obtained from experiments conducted at considerably higher temperatures and reactant concentrations than those of interest in polluted atmospheres.

In this paper, results are presented from experiments, conducted under near-atmospheric conditions, on heterogeneous reactions of oxides of nitrogen. A wide variety of solids are found to be capable of decomposing  $\text{NO}_2$ . This is especially true when the reaction mixture is humidified (40-50% relative humidity). In fact, some materials found to be unreactive in the absence of added moisture reacted readily when water vapor was added. In the case of  $\text{NO}$ , except for reactions over  $\text{MnO}_2$ , only minimal activity was observed, and it was concluded that heterogeneous reactions of this gas are unimportant in polluted atmospheres.

Products formed during the heterogeneous decomposition of  $\text{NO}_2$  consisted primarily of strongly adsorbed surface nitrogen compounds and gaseous  $\text{NO}$ .

Overall, the heterogeneous processes led to a substantial reduction of  $\text{NO}_x$  (i.e.,  $\text{NO} + \text{NO}_2$ ) in the gas phase.

Quantitatively, projection of our laboratory results for  $\text{NO}_2$  to the atmosphere leads to the conclusion that  $\text{NO}_2$  decomposition on the surface of airborne particles in polluted atmospheres can occur with a lifetime of  $\sim 0.5$  to 5 hours. This compares favorably with observed  $\text{NO}_2$  decay times of several hours (6,7) and suggests the potential importance of heterogeneous processes for the removal of  $\text{NO}_2$ . Moreover, although our results indicate only minimal heterogeneous activity toward  $\text{NO}$ , the latter species is rapidly converted to  $\text{NO}_2$  in polluted atmospheres (7,8). Consequently, heterogeneous processes could also be important in the removal of  $\text{NO}_x$  emitted as  $\text{NO}$ .



## SECTION 2

### EXPERIMENTAL

#### MATERIALS

Solids used in the present study are listed in Table 1, along with their BET surface areas. These solids were supported on various pyrex cylinders or helices ranging from  $\sim 1$  cm in diameter x 10 cm long to 3.2 cm in diameter x 40 cm long. The helices were constructed from 3-mm pyrex rod with  $\sim 3$  mm between loops. The appropriate cylinder or helix was prepared by spraying a fluid suspension of the desired solid (water, acetone, alcohol, or mixtures of these were used as the fluid carrier) onto the cylinder or helix and allowing the wet film to dry in air before use. Typically, the net weight of the dry film was several hundred milligrams. The coated cylinder or helix was inserted concentrically into one of two cylindrical flow reactors and further dried under vacuum ( $<10^{-2}$  Torr<sup>1</sup>) for 1 to 3 hours or in some cases overnight. (In the case of  $H_2SO_4$ , a cylinder was coated with the concentrated acid, inserted directly into the reactor, and used immediately without extensive evacuation.)

Gases used in these studies were obtained from Matheson. Gases were used as received, except for NO-N<sub>2</sub> or NO-Ar mixtures. The latter gases were passed through a molecular sieve column before use to decompose any residual NO<sub>2</sub>. Various gas mixtures were prepared or humidified through the use of procedures described elsewhere (9,10).

#### REACTORS

Two different cylindrical flow reactors were used in these studies (10,11). The reactors differed principally in their modes of reactant and product analysis. The first reactor (11), designated reactor F (fluorescence detection), was used for detailed rate studies of the heterogeneous

---

<sup>1</sup>Torr =  $1.33 \times 10^{-2}$  Newton/meter<sup>2</sup>

TABLE 1. SOLIDS STUDIED AND PHYSICAL ADSORPTION SURFACE AREAS\*

Material	Source	Area (m <sup>2</sup> /g)
Al <sub>2</sub> O <sub>3</sub> <sup>†</sup>	Analabs, activated alumina no. 214-77	196
Al <sub>2</sub> O <sub>3</sub>	J.T. Baker, no. 0537	233 ± 7 <sup>‡</sup>
Wood charcoal powder	Allied Chemical, no. 1567	40.7
Cement <sup>†</sup>	California Portland Cement	17.9
PbO	J.T. Baker, no. 2338 yellow powder	20.1
MnO <sub>2</sub>	ROC/RIC, MN-37	109 ± 10 <sup>‡</sup>
Fly ash	Western Coal Burning Power Plant	15.2
ZnO	New Jersey Zinc, SP500	22.2
Cu <sub>2</sub> O	ROC/RIC, CU-33 red 99%	5.5 ± 3.0 <sup>‡</sup>
Fe <sub>2</sub> O <sub>3</sub>	Commercial jeweler's rouge	27.3
Sand <sup>†</sup>	Baker and Adamson, no. 2171	7.3
V <sub>2</sub> O <sub>5</sub>	ROC/RIC V-15	14.1

\*BET measurements using N<sub>2</sub> at -196 C, except for the case of MnO<sub>2</sub> where CO<sub>2</sub> was used at -78C. The following materials were also used, but their BET areas were not measured: (NH<sub>4</sub>)<sub>2</sub>SO<sub>4</sub>, Al (powdered metal), CaO, PbCl<sub>2</sub>, crushed oleander leaves, H<sub>2</sub>SO<sub>4</sub>, and soil (loam).

†Crushed to a fine powder before use. Other materials used as received.

‡Errors derived from estimates of error in reading pressure devices, i.e., Matheson 0-760 and voltmeter used with pressure transducer plus an 0.01 V/min drift noted.

decomposition of  $\text{NO}_2$ . Generally,  $\text{NO}_2$ -Ar mixtures were used in this reactor. An argon ion laser (488 nm) excited  $\text{NO}_2$  fluorescence along the cylinder axis. This fluorescence was detected at right angles to the laser beam by a photomultiplier equipped with narrow slits. A narrow uncoated strip running the length of the cylinder on which the solid was supported permitted the fluorescence to reach the photomultiplier tube. The coated cylinder (with the uncoated strip) was mounted on a platform inside the reaction chamber. This platform was constructed such that the cylinder could be moved back and forth along the direction of the cylinder axis (11). This feature, along with the narrow laser excitation beam and the narrow slits on the photomultiplier, permitted the determination of  $\text{NO}_2$  concentration gradients along the cylinder axis. The latter data, in conjunction with a mathematical analysis of the system (11, 12), were used to obtain the gas-solid reaction rate constants.

In the second reactor (10), designated reactor A (absorption detection),  $\text{NO}_2$  was monitored by its optical absorption (480 nm) along the cylinder axis. A chopped dual beam optical scheme was used for this purpose. Unlike reactor F, the coated cylinder (or helix, which was also used in this reactor) was not movable, and spatial discrimination of  $\text{NO}_2$  along the cylinder axis was not obtained. However, other reactants or products (i.e., NO and  $\text{O}_2$ ) and inert gases (i.e.,  $\text{N}_2$  and Ar) could be analyzed before entry into or after exit from the cylinder. Reactant or product NO was determined through a chemiluminescent reaction with  $\text{O}_3$ , while gas chromatography was used for the other gases (10).

The effects of moisture and simulated solar ultraviolet and visible radiation could be determined in reactor A. Reaction mixtures were humidified through the use of techniques similar to those described by Cheng et al. (9) and Hedgpeth et al. (10). A bank of daylight-type fluorescent lights surrounding the (pyrex) reactor was used to simulate solar radiation. In the latter experiments, the coated helix was used, since this configuration allowed for a more even light distribution inside the chamber. Additional details on this system are given by Hedgpeth et al. (10), while the procedures used for data analysis are described by Siegel et al. (12).

## ANALYSIS OF SURFACE NITROGEN COMPOUNDS

In several experiments, the coated cylinders were removed from the reaction chamber upon completion of the experiment, washed with distilled water, and filtered, and the filtrate analyzed for  $\text{NO}_x^-$  (i.e.,  $\text{NO}_2^-$  or  $\text{NO}_3^-$ ). A wet chemical procedure or nitrate ion electrode (Beckman, model no. 39618) was used for  $\text{NO}_3^-$  analysis (12-13), while wet chemical techniques were employed for  $\text{NO}_2^-$  analysis (13). The latter test gives a positive result for both  $\text{NO}_2^-$  and gaseous  $\text{NO}_2$  dissolved in solution. Consequently, the  $\text{NO}_2^-$  test cannot distinguish between adsorbed  $\text{NO}_2$  and  $\text{NO}_2^-$ . An additional uncertainty in the analyses of  $\text{NO}_x^-$  lies in the possibility that  $\text{NO}_x^-$  could be formed from adsorbed  $\text{NO}_2$  during the washing procedures.

In some cases, these experiments were run for short periods of time to avoid poisoning heterogeneous activity. In these experiments, the solid was removed in segments, washed, and filtered, and the individual filtrates analyzed for  $\text{NO}_x^-$ .

## SECTION 3

### RESULTS

#### DECOMPOSITION OF $\text{NO}_2$ IN DRY REACTION MIXTURES

##### Reactivities of Charcoal, $\text{Al}_2\text{O}_3$ , and $\text{MnO}_2$

A series of experiments was conducted through the use of reactor F and  $\text{NO}_2$ -Ar mixtures to determine quantitatively the heterogeneous decomposition rates of  $\text{NO}_2$  over charcoal,  $\text{Al}_2\text{O}_3$ , and  $\text{MnO}_2$ . Earlier experiments in reactor A had demonstrated that this reaction readily occurs in  $\text{N}_2$ - $\text{O}_2$ -NO- $\text{NO}_2$  mixtures yielding surface nitrates, nitrites, and gaseous NO. Gas mixtures consisted of 0.05 to 5%  $\text{NO}_2$  in Ar, with total pressures of 1 to 100 Torr. The  $\text{NO}_2$  concentration, detected by laser-excited fluorescence, was measured as a function of distance along the axis of the cylindrical reactor.

Data from these experiments were analyzed through the use of model described by Stewart and Judeikis (11) and Siegel et al. (12). In this model, the rate of change of the  $\text{NO}_2$  concentration at the walls is written in terms of diffusion of gaseous  $\text{NO}_2$  to and from the walls of the coated cylinder, the gaseous flow rate through the cylinder, and the ratio  $k_r/k_c$ , where  $k_r$  is the rate constant for removal of  $\text{NO}_2$  from the gas phase and  $k_c$  is the gas-solid collision rate constant. (Thus,  $k_r/k_c$  is the fraction of gas-solid collisions leading to removal of  $\text{NO}_2$  from the gas phase.) Integration of the resulting differential equation yields a Bessel series solution for the spatial distribution of gaseous  $\text{NO}_2$  in the cylinder. This series reduces to a single exponential term for large distances along the cylinder axis.

Results from a typical experiment with charcoal are illustrated in Figure 1. The data shown by the solid curve in the figure were calculated through the use of experimental parameters and a value of 0.0016 for  $k_r/k_c$ . An example of the exponential decay with distance at large distances is illustrated in Figure 2 for data from an experiment with  $\text{MnO}_2$ . The solid

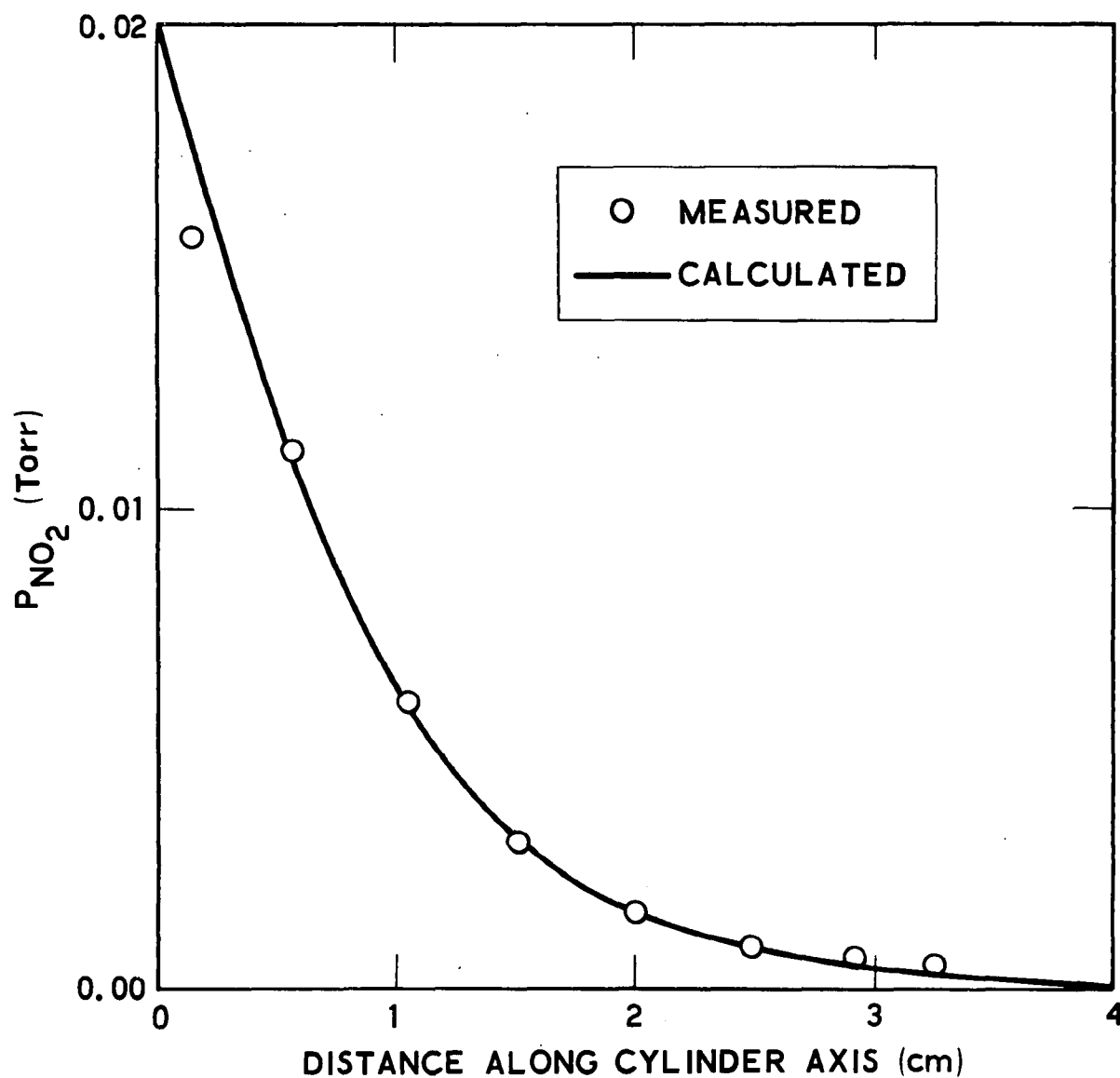


Figure 1. Decomposition of NO<sub>2</sub> over charcoal. Experimental conditions: 0.2% NO<sub>2</sub> in Ar (10 Torr total pressure),  $23 \pm 1$  C, 1.7 cm<sup>3</sup>/sec flow, and a cylinder radius of 0.95 cm.

curve in Figure 2 represents the limiting slope calculated for large distances through the use of the experimental parameters, a value of  $k_r/k_c$  of 0.0003, and the model described above.

Data from experiments in reactor F were analyzed through the use of the method indicated in Figure 2; i.e., the exponential decay with distance was fitted through the use of limiting slopes calculated from the model described by Stewart and Judeikis (11) and Siegel et al. (12). In general, slopes differing by about  $\pm 25\%$  from the best fitting slope would give noticeable deviations from the experimental limiting slope. Examples of experimental reproducibility for  $\text{NO}_2$  decomposition over charcoal as a function of cylinder radius, total pressure, and flow rate are given in Table 2. The average value of  $k_r/k_c$  for charcoal in these experiments was found to be  $1.6 \times 10^{-3}$  (standard deviation =  $\pm 0.5 \times 10^{-3}$ ). Results from similar experiments with  $\text{MnO}_2$  exhibited somewhat greater variations, and it is concluded that  $k_r/k_c = 0.3$  to  $3 \times 10^{-3}$ , whereas for  $\text{Al}_2\text{O}_3$  (Analabs) it is found that  $k_r/k_c = (3 \pm 1) \times 10^{-4}$ .

TABLE 2. DECOMPOSITION OF  $\text{NO}_2$  OVER CHARCOAL\*

Cylinder Radius (cm)	$P_{\text{total}}$ (Torr)	Flow Rate ( $\text{cm}^3/\text{sec}$ )	$10^3 \times \frac{k_r}{k_c}$
0.50	1.0	17.5	2.6
	9.9	25.0	1.2
	10.2	16.5	1.4
0.95	1.0	0.4	1.5
	1.0	0.4	1.0
	9.8	1.7	1.6
	10.3	1.7	1.6

\*Reaction mixture: 0.2%  $\text{NO}_2$  in A ( $23 \pm 1$  C).

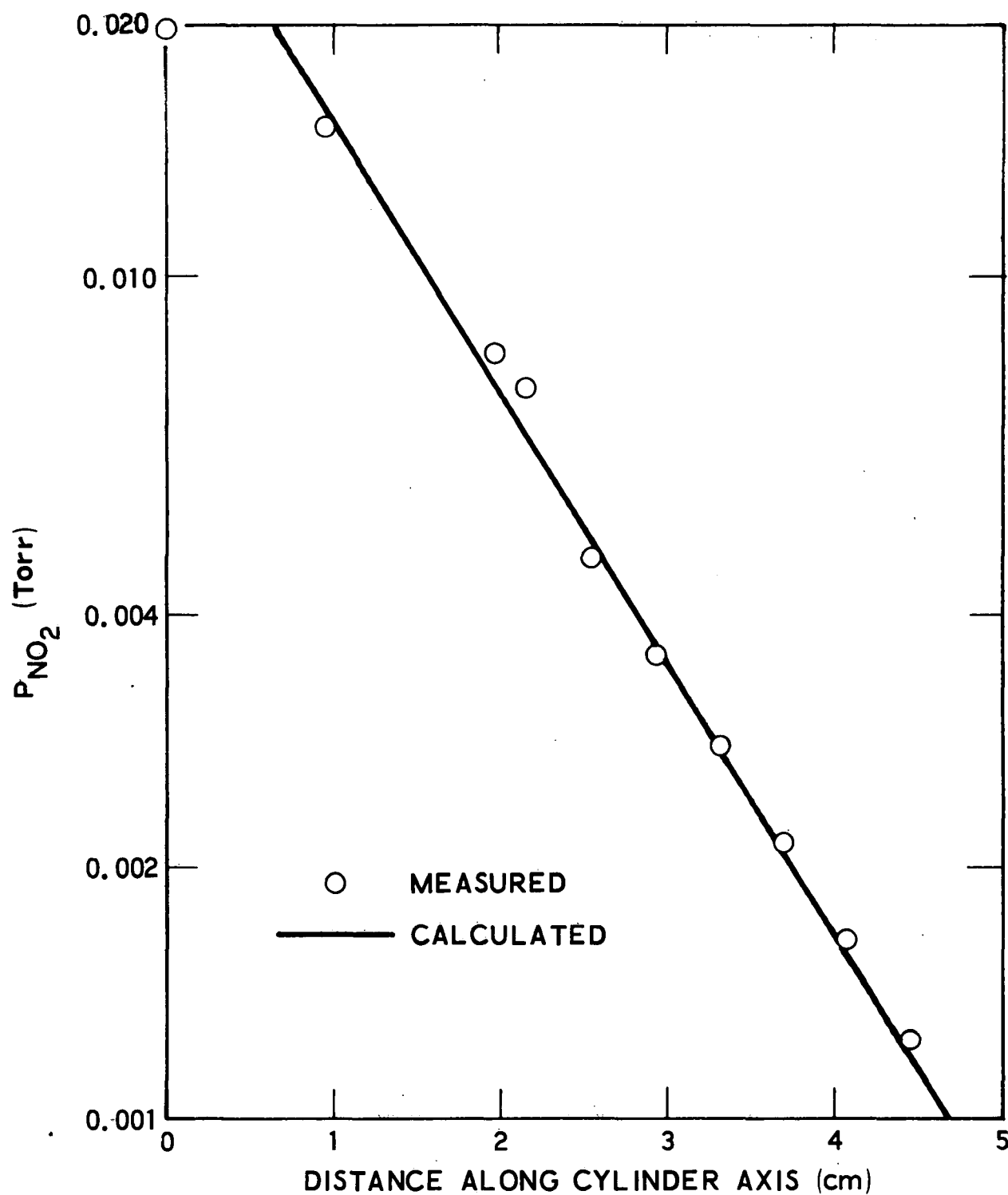


Figure 2. Decomposition of NO<sub>2</sub> over MnO<sub>2</sub>. Experimental conditions: 0.2% NO<sub>2</sub> in Ar (10 Torr total pressure),  $23 \pm 1$  C, 1.0 cm<sup>3</sup>/sec flow, and a cylinder radius of 0.95 cm.



### Additional Experiments in Reactor A

An additional sequence of experiments with dry  $\text{NO}_2\text{-N}_2$  or  $\text{NO}_2\text{-Ar}$  mixtures was carried out in reactor A. The purpose of these experiments was to screen other solids for reactivity toward  $\text{NO}_2$ , analyze gaseous and adsorbed reaction products, measure overall capacities for reaction, and examine the effects of simulated solar radiation. Because of pressure and flow rate limitations, however, only minimum reactivities could be determined for solids that efficiently removed  $\text{NO}_2$ . This was because, for  $k_r/k_c \geq 10^{-4}$ , reactions were limited by diffusion of gaseous  $\text{NO}_2$  to the cylinder walls in this system.

In addition to those materials discussed in the preceding section, the following solids were found to exhibit substantial reactivity ( $k_r/k_c \geq 10^{-4}$ ) toward  $\text{NO}_2$  decomposition:  $\text{Al}_2\text{O}_3$  (Baker), cement,  $\text{PbO}$ , fly ash, and  $\text{CaO}$ . The remaining materials in Table 1 exhibited only minimal activity ( $k_r/k_c < 3 \times 10^{-7}$ ) or no activity within experimental error toward dry  $\text{NO}_2$  reaction mixtures.

Results from representative experiments in reactor A are illustrated in Figure 3. These results are from experiments in which glass helices (3.2 cm in diameter x 40 cm long) were used to support  $\text{PbO}$  and cement. In addition, a 1-mil sheet of DuPont Kapton was placed between the fluorescent lamps and reactor to filter wavelengths responsible for direct photolysis of  $\text{NO}_2$  (10).

Experimentally, dry nitrogen was passed through the chamber at the desired flow and pressure until the gas flow stabilized. Then valves were rapidly switched to admit  $\text{NO}_2\text{-N}_2$  mixtures at the same pressures and flows. This procedure avoided pressure surges in the system and required only a few minutes for the  $\text{NO}_2\text{-N}_2$  flow to stabilize (see blank run in Figure 3).

In the case of  $\text{PbO}$  and cement, the initial nonzero values for the average  $\text{NO}_2$  pressured after stabilization are due to the reaction mixtures filling the space between the gas inlet and leading edge of the helices, as well as partially penetrating into the helices before  $\text{NO}_2$  diffuses to the helix walls and reacts. Over long periods of time ( $\sim 400$  min in the experiments illustrated), the  $\text{NO}_2$  concentrations slowly increased as the activities of the solids gradually diminished, and ultimately ( $t > 400$  min) reached the

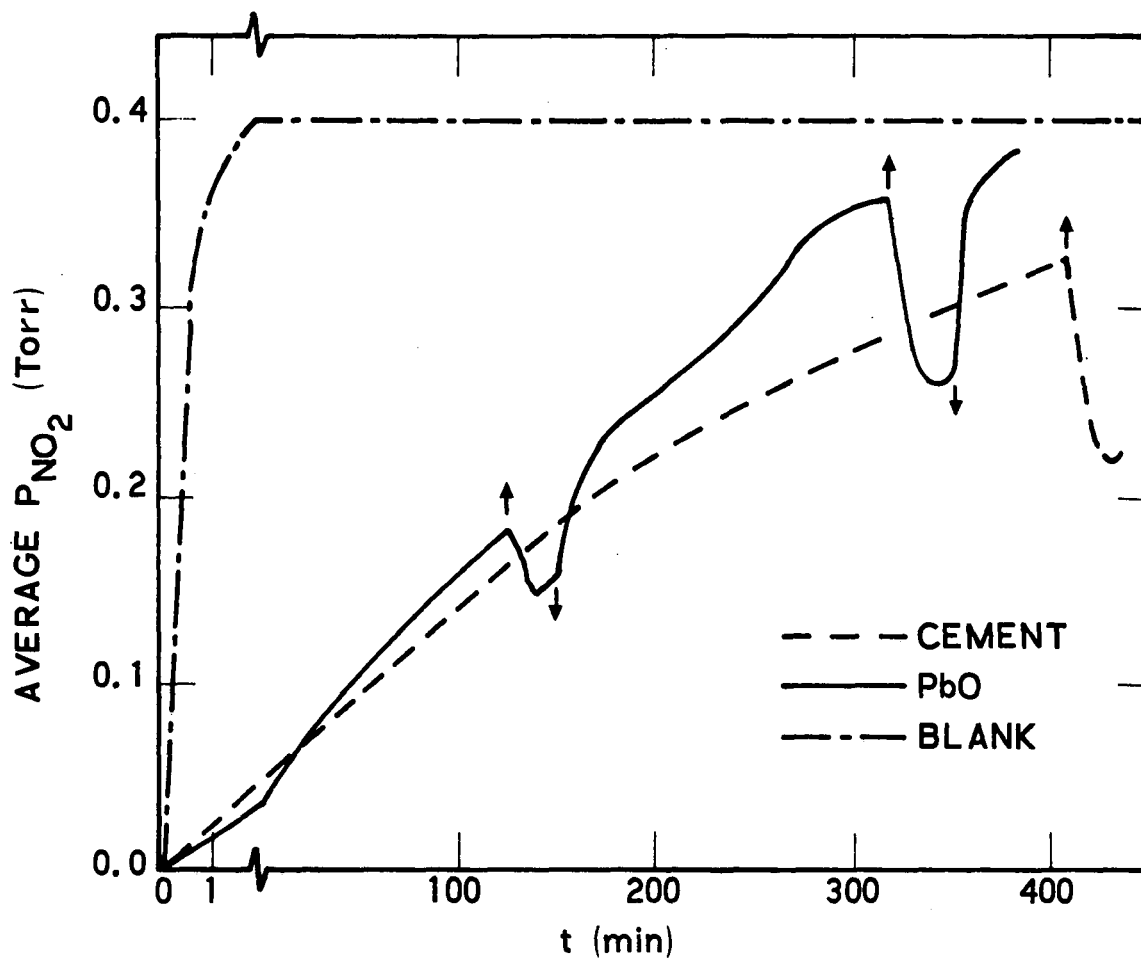


Figure 3. Decomposition of  $\text{NO}_2$  over PbO and cement. Experimental conditions: 0.2%  $\text{NO}_2$  in  $\text{N}_2$  [total pressures of 191 Torr (PbO) and 200 Torr (cement)],  $23 \pm 1^\circ\text{C}$ , and flow rates of  $9.5 \text{ cm}^3/\text{sec}$  (PbO) and  $11.6 \text{ cm}^3/\text{sec}$  (cement). The remaining curve in the figure is for a blank experiment conducted in the absence of added solids with the same experimental conditions as for PbO. Arrows indicate where fluorescent lamps ( $\sim 3$  equivalent suns) were turned on (+) or off (-).

levels obtained in the absence of added solids when the activities of the PbO and cement were completely destroyed (not shown).

From the flow rates, weights of solids, and time to poisoning, the capacities of the solids to destroy  $\text{NO}_2$  can be calculated. The results for the experiments discussed above, as well as experiments in which other solids were investigated are given in the first column of Table 3. Once poisoned, exposure of the solid to vacuum for periods up to several hours did not restore any substantial activity. Also, introduction of  $\text{O}_2$  during or after the experimental had little effect on the results, which indicated poisoning was not due to depletion of surface oxygen.

Exposure of samples to visible light during experiments led to brief decreases or increases in  $\text{NO}_2$ , which suggested a slight restoration of solid activity in the former case, or photodesorption of adsorbed  $\text{NO}_2$  in the latter. However, these changes were short-lived (Figure 3) and had little effect on the overall activity or capacity of the solid. Exposure to visible light after the solid had been poisoned frequently led to brief, large increases in  $\text{NO}_2$ , probably because of photodesorption. Here also, the overall effects on reactivity and capacity were small.

### Reaction Products

In selected experiments, solids were removed from the reactor upon completion of the experiment, washed with distilled water, and filtered, and the filtrate analyzed for  $\text{NO}_x^-$  (see Section 2 for discussion of uncertainties). Results from these experiments are given in Table 4. The results indicate that both  $\text{NO}_2^-$  and  $\text{NO}_3^-$  are formed, the dominant specie depending on the solid used. The identity of the  $\text{NO}_x^-$  formed appeared to be independent of the length of time the experiment was run.

In the case of  $\text{Al}_2\text{O}_3$ , the Analabs material gave predominantly  $\text{NO}_2^-$ , while the Baker  $\text{Al}_2\text{O}_3$  gave mostly  $\text{NO}_3^-$ . Elemental and x-ray analysis of these two solids indicated slight differences. Thus, elemental analysis gave higher percentages of Si, Fe, and Na in the Analabs material (0.1 - 0.3% versus 0.002 - 0.08%). In addition, although the dominant x-ray patterns from both materials were similar (boehmite), the Analabs material gave several extra (unidentified) peaks not observed for the Baker  $\text{Al}_2\text{O}_3$ .

TABLE 3. DECOMPOSITION OF  $\text{NO}_2$  OVER VARIOUS SOLIDS<sup>\*†</sup>

	Dry Reaction Mixtures		Humidified Reaction Mixtures <sup>††</sup>	
	Capacity	$\text{NO}_x^-$ Formed	Capacity	$\text{NO}_x^-$ Formed
PbO	0.05	-	>0.23	-
Cement	0.05	-	>0.37	-
$\text{Al}_2\text{O}_3$ <sup>§</sup>	$0.07 \pm 0.02$	$0.03 \pm 0.01$	$0.21 \pm 0.01$	$0.11 \pm 0.01$
Charcoal	$0.12 \pm 0.03$	$0.03 \pm 0.01$	$0.24 \pm 0.09$	$0.09 \pm 0.05$
$\text{MnO}_2$	0.04		>0.41	

\* Capacities refer to the grams of  $\text{NO}_2$  decomposed per gram of solid, while  $\text{NO}_x^-$  formed refers to the grams of  $\text{NO}_2$  converted to surface  $\text{NO}_x^-$  per gram of solid.

† Uncertainties are standard deviations from 3 to 5 experiments. Results expressed without uncertainties are from single experiments (see Figure 6).

†† 44% relative humidity

§ Baker.

TABLE 4. ANALYSIS OF SURFACE NITROGEN COMPOUNDS

Solid	Surface Nitrogen Compounds			
	$\text{NO}_3^-$	$\text{NO}_2^-$	Total as $\text{NO}_2^-$ (mg)	$\text{NO}_2^-$ Lost
$\text{Al}_2\text{O}_3^*$	Small	Large	24	24
			19	14
			0.8	1.0
$\text{Al}_2\text{O}_3^\dagger$	Large	Small	-	-
Charcoal	Large	Small	-	-
$\text{MnO}_2$	Large	Small	-	-
$\text{PbO}$	Small	Large	-	-

\* Analabs.

 $^\dagger$  Baker.

Experiments were also conducted to quantitatively determine  $\text{NO}_x^-$ . Experiments run for short periods of time to avoid poisoning indicated a quantitative conversion of  $\text{NO}_2$  to  $\text{NO}_x^-$ . This is illustrated for  $\text{Al}_2\text{O}_3$  in the last two columns of Table 4. The  $\text{NO}_2$  lost was determined from the gas pressures, flow rates, and duration of the experiment. In several of these experiments, adsorbed  $\text{NO}_x^-$  was analyzed as a function of distance along the cylinder. Results from a typical experiment are shown in Figure 4. After the experiment, the  $\text{Al}_2\text{O}_3$  was removed in sections, and the  $\text{NO}_x^-$  was analyzed in each section. The model described by Stewart and Judeikis (11) and Siegel et al. (12) was used to determine the calculated concentration profile, which was normalized through the use of the gas flow data and under the assumption that  $k_r/k_c \geq 10^{-4}$ , which is the diffusion limit in this experiment. Thus, the calculated and experimental results may be quantitatively compared. The major discrepancy, which occurs near  $z = 0$ , is probably due to edge effects.

Additional experiments were conducted for longer periods of time to investigate changes that might occur as the solid activity poisons. Results from these experiments are given in the third column of Table 3 and indicate that the  $\text{NO}_2 \rightarrow \text{NO}_x$  conversion becomes less than quantitative. In order to establish a material balance for the  $\text{NO}_2$  lost, several experiments were conducted with  $\text{Al}_2\text{O}_3$  (Baker) and  $\text{MnO}_2$  to determine if gaseous products were formed. Results from one such experiment for  $\text{NO}_2$  decomposition over  $\text{Al}_2\text{O}_3$  are shown in Figure 5. The production of gaseous NO (measured in the exit stream) is apparent. Integration of the NO produced and  $\text{NO}_2$  lost indicates a 62% conversion of  $\text{NO}_2$  to NO. The remaining 38% can be accounted for, to within experimental error, by  $\text{NO}_x^-$  formed on the  $\text{Al}_2\text{O}_3$  surface. Similar results were obtained for  $\text{MnO}_2$  with a 71%  $\text{NO}_2 \rightarrow \text{NO}$  conversion. In the case of  $\text{MnO}_2$ , a distinct induction period was observed for NO formation even though  $\text{NO}_2$  was destroyed. The latter observation may be due in part to removal of product NO by  $\text{MnO}_2$  (see Section 3--Reactivity of NO).

#### DECOMPOSITION OF $\text{NO}_2$ IN MOIST REACTION MIXTURES

The effects of moisture on the decomposition of  $\text{NO}_2$  were quite dramatic and are illustrated in Figure 6. In the experiments illustrated, only the first several centimeters of the cylinder were coated with the indicated solids. Dry reaction mixtures were passed through the chamber until

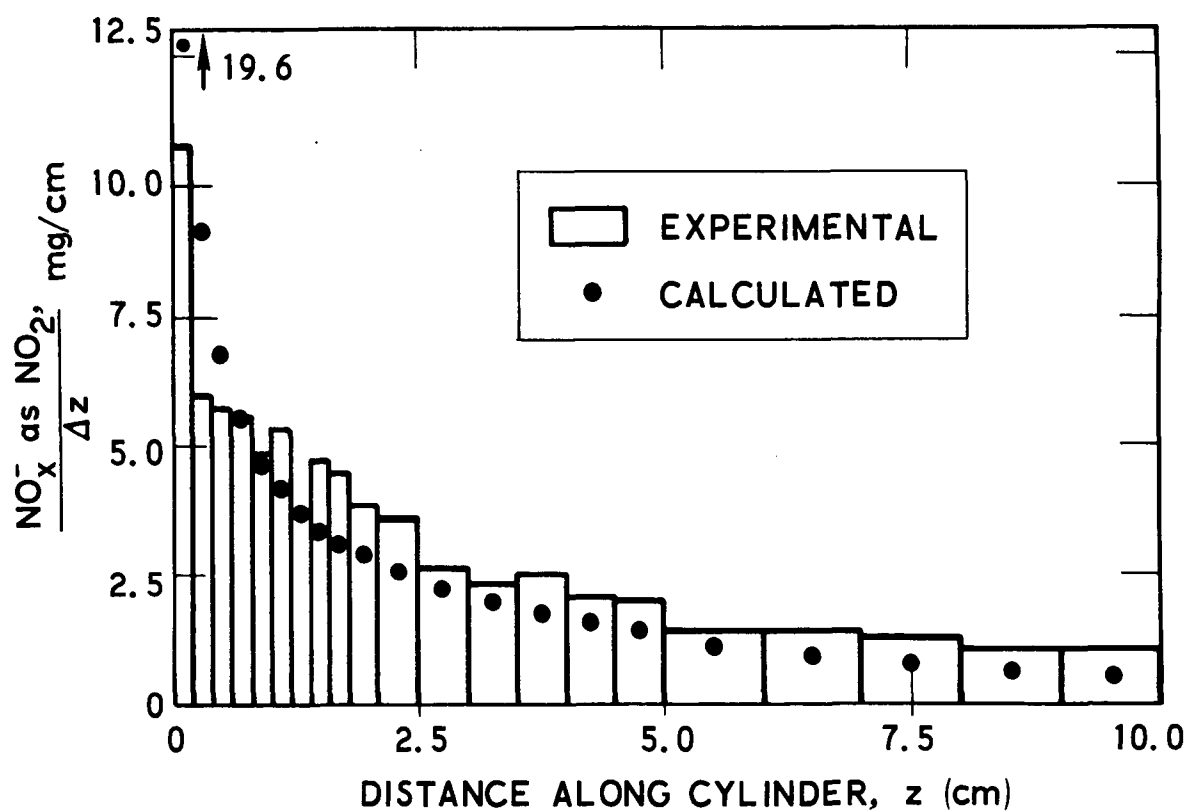


Figure 4. Surface nitrogen compounds measured after  $\text{NO}_2$  decomposition over  $\text{Al}_2\text{O}_3$  (Baker). Experimental conditions: 0.2%  $\text{NO}_2$  in  $\text{N}_2$  (700 Torr total pressure),  $23 \pm 1$  C, flow rate =  $10 \text{ cm}^3/\text{sec}$ , and cylinder radius = 2.0 cm.

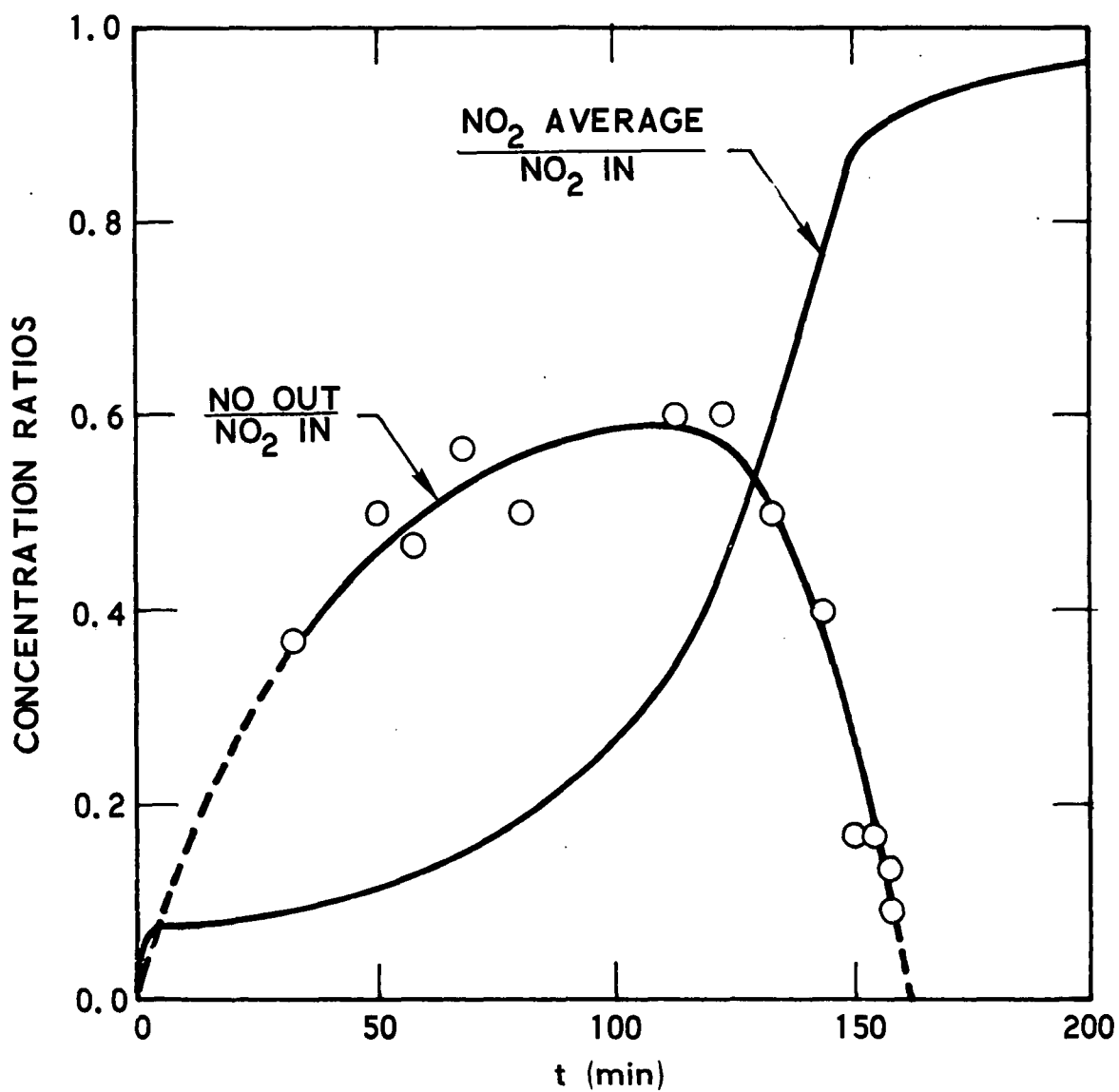


Figure 5. Decomposition of  $\text{NO}_2$  over  $\text{Al}_2\text{O}_3$  (Baker).  
 Experimental conditions: 0.05%  $\text{NO}_2$  in  $\text{N}_2$   
 (180 Torr total pressure),  $23 \pm 1^\circ \text{C}$ , flow  
 rate =  $9.2 \text{ cm}^3/\text{sec}$ , and cylinder radius =  
 2.0 cm.



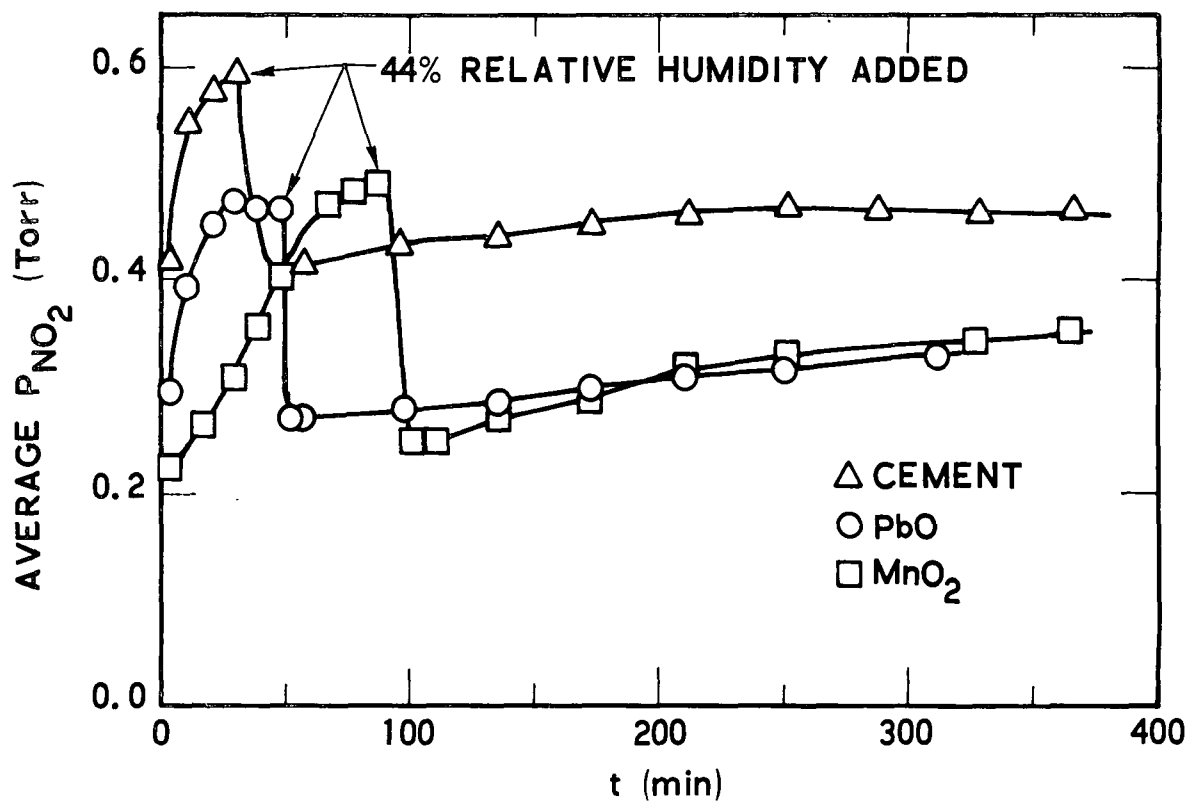


Figure 6. Decomposition of NO<sub>2</sub> over selected solids. Effects of added moisture. Experimental conditions: 0.2% NO<sub>2</sub> in Ar (~200-300 Torr total pressures), 23 ± 1 C, flow rates ≈ 10 cm<sup>3</sup>/sec, and cylinder radius = 2.0 cm.

reactivity was destroyed. At that point moisture was added (44% relative humidity), and the activity was restored. Separate experiments in the absence of added solids indicated gas phase reactions between  $\text{NO}_2$  and  $\text{H}_2\text{O}$  were unimportant below 50% relative humidity. From Figure 6, it will be noted that the total activity (before poisoning) is substantially increased when moisture is added. Similar results were obtained when moisture was present initially in the reaction mixture. Quantitative values for capacities in moist systems are given in the last two columns of Table 3. Diffusion limited reaction rates were obtained in the presence of moisture ( $k_r/k_c \geq 10^{-4}$ ) for the first seven materials listed in Table 1 and for  $\text{CaO}$ , all of which were reactive in dry systems.

An equally significant result was that materials found to be unreactive in the absence of moisture reacted readily when moisture was added (44% relative humidity). The following values were measured for  $k_r/k_c$  in these experiments:  $\geq 10^{-4}$  ( $\text{ZnO}$ ),  $3 \times 10^{-5}$  ( $\text{Cu}_2\text{O}$ ,  $\text{Fe}_2\text{O}_3$ ),  $1 \times 10^{-5}$  (sand), and  $1 \times 10^{-6}$  [ $\text{V}_2\text{O}_5$ ,  $(\text{NH}_4)_2\text{SO}_4$ ,  $\text{H}_2\text{SO}_4$ ]. The remaining materials in Table 1 were not examined in these experiments.

Glass filter paper of the type used in high-volume samplers for collecting airborne particles was also examined. While this material was unreactive with dry  $\text{NO}_2$ - $\text{N}_2$  mixtures, the addition of moisture led to extensive decomposition of  $\text{NO}_2$  ( $k_r/k_c \geq 10^{-4}$ ). This could have serious consequences in the interpretation of particulate data if surface  $\text{NO}_x^-$  compounds are formed. Some discrepancies between particles collected on various types of filters have been noted (14).

In one case ( $\text{Fe}_2\text{O}_3$ ), reactivity was examined as a function of relative humidity (rh). The results obtained for  $k_r/k_c$  were:  $< 10^{-7}$  (0-7% rh),  $\sim 5 \times 10^{-6}$  (14% rh),  $\sim 1.6 \times 10^{-5}$  (28% rh), and  $\sim 3 \times 10^{-5}$  (44% rh). Attempts to conduct experiments at higher relative humidities were unsuccessful because of gas phase (or wall) reactions involving  $\text{NO}_2$  and  $\text{H}_2\text{O}$ .

The increased reactivity and capacity in the presence of moisture led to the exploration of the possibility that surface nitrogen compounds formed in the presence of water might volatilize as the corresponding acids. In experiments with  $\text{MnO}_2$  and  $\text{Al}_2\text{O}_3$  (Baker), effluent gas from the reactor was

bubbled through a water solution, and the solution analyzed at intervals for  $\text{NO}_3^-$  and pH. (Under the experimental conditions,  $\text{NO}_2$  was completely destroyed in transit through the reactor being converted, in part, to gaseous NO.) In the case of  $\text{MnO}_2$ ,  $\text{NO}_3^-$  was observed even in dry reaction mixtures and increased when moisture was added. (Separate experiments bubbling NO through the water gave a negative  $\text{NO}_3^-$  test). In the presence of moisture, the  $\text{NO}_3^-$  analysis and pH indicate that ~2 to 3% of the  $\text{NO}_2$  lost is ultimately converted to volatile  $\text{HNO}_3$  in the effluent stream. For  $\text{Al}_2\text{O}_3$ , no  $\text{NO}_3^-$  was observed in the effluent stream.

#### REACTIVITY OF NO

A number of experiments was conducted in reactor A with  $\text{NO-O}_2\text{-N}_2$  mixtures to determine the reactivity of NO toward various solids. The conditions of these experiments were such that ~10 to 20% of the NO was converted to  $\text{NO}_2$  during passage through the reactor by the termolecular gas phase reaction between NO and  $\text{O}_2$  (7-8). Several of the materials listed in Table 1, notably  $\text{V}_2\text{O}_5$  and  $\text{ZnO}$ , appeared to exhibit some activity toward oxidation (photo-oxidation in the case of  $\text{ZnO}$ ) of NO to  $\text{NO}_2$ , as evidenced by increased  $\text{NO}_2$  yields. However,  $k_r/k_c \approx 10^{-7}$  for these cases. In the case of  $\text{MnO}_2$ , charcoal, and  $\text{Al}_2\text{O}_3$ ,  $\text{NO}_2$  yields were sharply decreased. Separate experiments with  $\text{NO-N}_2$  mixtures indicated that, except for  $\text{MnO}_2$ , this decrease was due to  $\text{NO}_2$ -solid interactions and not NO-solid interactions. For  $\text{MnO}_2$ , both NO and  $\text{NO}_2$  were reactive with  $k_r/k_c \geq 10^{-4}$ . The remaining materials listed in Table 1 exhibited no reactivity toward NO to within experimental error and  $k_r/k_c < 10^{-7}$ .

Additional experiments were carried out with humidified (44% relative humidity)  $\text{NO-N}_2$  mixtures to determine the effects of moisture on reactivities. The materials examined were  $\text{Al}_2\text{O}_3$ , charcoal,  $\text{ZnO}$ , and  $\text{V}_2\text{O}_5$ . Unlike the case of  $\text{NO}_2$ , moisture had no effect on the NO-solid interactions to within the limits of experimental detectability ( $k_r/k_c < 10^{-7}$ ).

## SECTION 4

### DISCUSSION AND CONCLUSIONS

The results for  $\text{NO}_2$  suggest that this pollutant could be heterogeneously destroyed in the atmosphere on a wide variety of airborne solids likely to be found in urban environments. The heterogeneous decomposition is greatly facilitated by the presence of moisture. In fact, many solids that were unreactive in the absence of moisture readily decomposed  $\text{NO}_2$  when water vapor was added. The striking effects of water suggest the involvement of surface OH groups in the heterogeneous processes.

Initially, the decomposition reactions quantitatively convert  $\text{NO}_2$  to adsorbed  $\text{NO}_x^-$ . With time, the conversion becomes less than quantitative, and gaseous NO is formed. Overall, ~20 to 30% of the  $\text{NO}_2$  lost is converted to adsorbed  $\text{NO}_x^-$ . Although volatilized  $\text{HNO}_3$  was observed in one case ( $\text{MnO}_2$ ), this product accounted for only ~2 to 3% of the  $\text{NO}_2$  lost. The possibility exists that  $\text{HNO}_2$  or  $\text{HNO}_3$  formed in the presence of moisture could react with a number of the oxides investigated in this study. Solution of the metal ions and reactions in surface water films would then be possible. A similar suggestion has been made for oxidation of  $\text{SO}_2$  to  $\text{H}_2\text{SO}_4$  in the presence of moisture over various solids (15).

Based on the initial reactivities observed in these studies, it is estimated that fresh aerosol in an urban atmosphere could remove  $\text{NO}_2$  with a lifetime of 1/2 to 5 hours. This projected lifetime is based on the model described by Judeikis and Siegel (5) and assumes a particle loading of  $100 \mu\text{g}/\text{m}^3$  and the reactivities measured in these experiments (e.g., if it is assumed that particles had the same reactivity as charcoal,  $\text{MnO}_2$ , or  $\text{Al}_2\text{O}_3$ , the calculated particle limited half-lives are 1, 1/2 to 5, and 5 hours respectively). The projected lifetimes could be shorter in the presence of moisture. As the aerosols age, the net removal of  $\text{NO}_2$  is formed as the

the reaction continues. The latter species is rapidly converted to  $\text{NO}_2$  in urban atmospheres during daylight hours (8).

The projected particle limited lifetimes compare favorably with observed diurnal variations in  $\text{NO}_x$  (6-7). They are longer than the noontime photolytic lifetime of 3 min for  $\text{NO}_2$  in the atmosphere (8); however, the heterogeneous processes lead to a net reduction in oxidant ( $\text{NO}_2 + \text{O}_3$ ), as well as  $\text{NO}_x$ , while the photolytic process does not. Moreover, since the photolytic process is not operable during the night, heterogeneous reactions could be the dominant nighttime sink for  $\text{NO}_2$ .

Only airborne particulate matter has been considered in our modeling. Consideration of ground-level surfaces could greatly enhance total reactivity. Moreover, reactions taking place on the latter surfaces could lead to concentration gradients near the ground, depending upon the amount of transport and mixing taking place. These gradients could be significant in accurately assessing pollution-related health hazards.

Finally, except for  $\text{MnO}_2$ , NO exhibits only minimal activity toward solids examined in this study. Based on quantitative rate measurements, it is concluded that heterogeneous atmospheric processes of NO are probably unimportant. However, as noted earlier, NO is rapidly converted to  $\text{NO}_2$  in urban atmospheres (8), and heterogeneous removal of the latter product could act as the ultimate sink for  $\text{NO}_x$  emitted as NO.

## REFERENCES

1. Johnstone, H.F., and D.R. Coughanowr. Adsorption of Sulfur Dioxide from Air. *Ind. Eng. Chem.*, 50:1169-1172, 1958.
2. Urone, P., H. Lutsep, C.M. Noyes, and J.F. Parcher. Static Studies of Sulfur Dioxide Reactions In Air. *Environ. Sci. Technol.*, 2:611-618, 1968.
3. Matteson, M.J., W. Stöber, and H. Luther. Kinetics of the Oxidation of Sulfur Dioxide by Aerosols of Manganese Sulfate. *Ind. Eng. Chem. Fundamentals*, 8:677-687, 1969.
4. Carabine, M.D. Interactions in the Atmosphere of Droplets and Gases. *Chem. Soc. Rev.*, 1:411-432, 1972.
5. Judeikis, H.S., and S. Siegel. Particle-Catalyzed Oxidation of Atmospheric Pollutants. *Atmospheric Environment*, 7:619-631, 1973.
6. Pitts, J.N. Environmental Appraisal: Oxidants, Hydrocarbons, and Oxides of Nitrogen. *J. Air Pollut. Control Ass.*, 19:658-667, 1969.
7. Altshuller, A.P., and J. Bufalini. Photochemical Aspects of Air Pollution: A Review. *Photochem. Photobiol.*, 4:97-146, 1965.
8. Shuck, E.A., and E.R. Stephens. Oxides of Nitrogen. In: *Advances in Environmental Sciences*, Vol.1, J.N. Pitts and R.L. Metcalf, eds. Wiley-Interscience, New York, New York, 1969. pp. 73-118.
9. Cheng, R.T., J.O. Frohlinger, and M. Corn. Aerosol Stabilization for Laboratory Studies of Aerosol-Gas Interactions. *J. Air Pollut. Control Ass.*, 21:138-142, 1971.
10. Hedgpeth, H., S. Siegel, T. Stewart, and H.S. Judeikis. Cylindrical Flow Reactor for the Study of Heterogeneous Reactions of Possible Importance in Polluted Atmospheres. *Rev. Sci. Instrum.*, 45(3): 344-347, 1972.
11. Stewart, T.B., and H.S. Judeikis. Measurements of Spatial Reactant and Product Concentrations in a Flow Reactor Using Laser-Induced Fluorescence. *Rev. Sci. Instrum.*, 45(12):1542-1545, 1974.
12. Siegel, S., H.S. Judeikis, and C. Badcock. The Role of Solid-Gas Interactions in Air Pollution. EPA-650/3-74-007, U.S. Environmental Protection Agency, Washington, D.C., 1974.

13. Feigl, F. Spot Test in Inorganic Analysis. Ed. 5. El Sevier Publishing Co., New York, New York, 1958. pp. 326-332.
14. Muller, P.K., S. Twiss, and G. Sanders. Selection of Filter Media: An Annotated Outline. Paper presented before 13th Conference on Methods Air Pollution and Industrial Hygiene Studies, Berkeley, California, October 30-31, 1972.
15. Foster, P.M. The Oxidation of Sulphur Dioxide in Power Station Plumes. Atmospheric Environment, 3:157-175, 1969.

<b>TECHNICAL REPORT DATA</b> <i>(Please read Instructions on the reverse before completing)</i>		
1. REPORT NO. EPA-600/3-77-028	2.	3. RECIPIENT'S ACCESSION NO.
4. TITLE AND SUBTITLE HETEROGENEOUS REACTIONS OF NITROGEN OXIDES IN SIMULATED ATMOSPHERES	5. REPORT DATE March 1977	
	6. PERFORMING ORGANIZATION CODE	
7. AUTHOR(S) H.S. Judeikis, S. Siegel, T.B. Stewart and H.R. Hedgpeth	8. PERFORMING ORGANIZATION REPORT NO. ATR-75(7441)-2	
9. PERFORMING ORGANIZATION NAME AND ADDRESS The Aerospace Corporation P.O. Box 92957 Los Angeles, California 90245	10. PROGRAM ELEMENT NO. 1AA603 (1AA008)	
	11. CONTRACT/GRANT NO. Grant No. 802687	
12. SPONSORING AGENCY NAME AND ADDRESS Environmental Sciences Research Laboratory Office of Research and Development U.S. Environmental Protection Agency Research Triangle Park, North Carolina 27711	13. TYPE OF REPORT AND PERIOD COVERED Interim 11/73-11/76	
	14. SPONSORING AGENCY CODE EPA/600/09	
15. SUPPLEMENTARY NOTES		
16. ABSTRACT  A laboratory study has been conducted on heterogeneous reactions of nitrogen dioxide and nitric oxide to evaluate their potential role in reaction in polluted urban atmosphere. The results of this study suggest that nitrogen dioxide decomposes on a wide variety of solids likely to be found in urban environments. Measured reaction rates indicate these processes can be important in the atmosphere. Humidification of reaction mixtures leads to increased reactivities. It is concluded that heterogeneous reactions in the atmosphere are unimportant for the oxidation of nitric oxide.		
17. KEY WORDS AND DOCUMENT ANALYSIS		
a. DESCRIPTORS	b. IDENTIFIERS/OPEN ENDED TERMS	c. COSATI Field/Group
*Air pollution *Nitrogen oxides Aerosols *Environmental simulation		13B 07B 07D 14B
18. DISTRIBUTION STATEMENT  RELEASE TO PUBLIC	19. SECURITY CLASS (This Report) UNCLASSIFIED	21. NO. OF PAGES 32
	20. SECURITY CLASS (This page) UNCLASSIFIED	22. PRICE